An untargeted thermogravimetric analysis-Fourier transform infrared-gas chromatography-mass spectrometry approach for plastic polymer identification

Nel, Holly A.; Chetwynd, Andrew J.; Kelly, Catherine A.; Stark, Christopher; Valsami-Jones, Eugenia; Krause, Stefan; Lynch, Iseult

DOI:
10.1021/acs.est.1c01085

Document Version
Publisher's PDF, also known as Version of record

Citation for published version (Harvard):
Nel, HA, Chetwynd, AJ, Kelly, CA, Stark, C, Valsami-Jones, E, Krause, S & Lynch, I 2021, 'An untargeted thermogravimetric analysis-Fourier transform infrared-gas chromatography-mass spectrometry approach for plastic polymer identification', *Environmental Science & Technology*, vol. 55, no. 13, pp. 8721-8729. https://doi.org/10.1021/acs.est.1c01085

Environmental Science & Technology

pubs.acs.org/est

Article

An Untargeted Thermogravimetric Analysis-Fourier Transform Infrared-Gas Chromatography-Mass Spectrometry Approach for Plastic Polymer Identification

Holly A. Nel,*[,‖] Andrew J. Chetwynd,[‖] Catherine A. Kelly, Christopher Stark, Eugenia Valsami-Jones, Stefan Krause, and Iseult Lynch

Cite This: https://doi.org/10.1021/acs.est.1c01085

Read Online

ACCESS | Metrics & More | Article Recommendations | Supporting Information

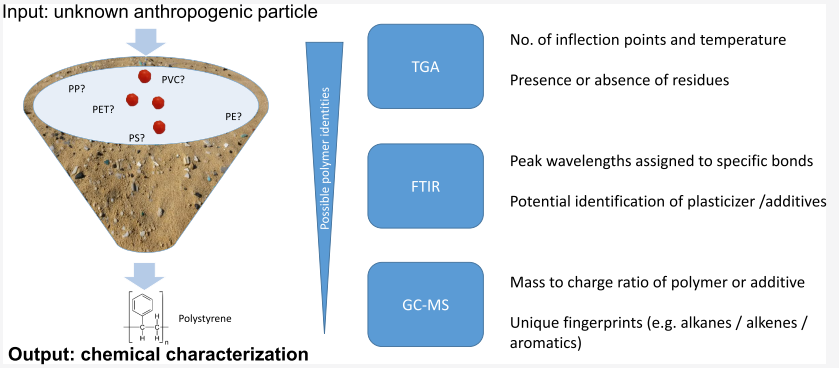

ABSTRACT: Reliable chemical identification of specific polymers in environmental samples represents a major challenge in plastic research, especially with the wide range of commercial polymers available, along with variable additive mixtures. Thermogravimetric analysis-Fourier transform infrared-gas chromatography-mass spectrometry (TGA-FTIR-GC-MS) offers a unique characterization platform that provides both physical and chemical properties of the analyzed polymers. This study presents a library of 11 polymers generated using virgin plastics and post-consumer products. TGA inflection points and mass of remaining residues following pyrolysis, in some cases, proved to be indicative of the polymer type. FTIR analysis of the evolved gas was able to differentiate between all but polypropylene (PP) and polyethylene (PE). Finally, GC-MS was able to differentiate between the unique chemical fingerprints of all but one polymer in the library. This library was then used to characterize real environmental samples of mesoplastics collected from beaches in the U.K. and South Africa. Unambiguous identification of the polymer types was achieved, with PE being the most frequently detected polymer and with South African samples indicating variations that potentially resulted from aging and weathering.

KEYWORDS: *mass spectrometry, thermogravimetric analysis, thermal analysis, pyrolysis, plastic, additives, plasticizers*

INTRODUCTION

Widespread contamination of the environment by plastic items has been documented by a large number of studies. Using the physical and chemical properties of plastic materials extracted from the environment, researchers are able to inform mitigation strategies, such as legislative action and industrial reform.[1] Additionally, items detected in the environment with an associated polymer identity can be used to trace major source inputs and identify long-term sinks. Modeling major sinks and hotspots globally through understanding how dominant polymers behave in the environment is useful to help identify vulnerable ecosystems associated with plastic exposure.[2,3] Chemical characterization is a typical reporting standard;[4] however, particles are often broadly assigned to a polymer type without providing details regarding variations in individual chemical structures. Given the wide array of plastics currently commercially available, along with the multiple additives (e.g., plasticizers, lubricants, and pigments) incorporated to improve plastic performance and functionality, a detailed chemical fingerprint would go a long way to improve our understanding of plastic sources and degradation and leaching rates.[5]

Fourier transform infrared (FTIR) and Raman spectroscopies are currently the most widely used tools for the

Received: February 15, 2021
Revised: May 24, 2021
Accepted: May 24, 2021

identification of meso- (particles between 1 and 10 mm) and microplastics (particles ≤ 1 mm), with most of the studies employing a manual preselection step followed by chemical characterization of a subset of individual particles.[6] Although chemical verification reduces the risk of misinterpretation of visually identified suspected plastic particles,[7] the manual preselection step can lead to an under-representation of ambiguous particles and thus introduce bias caused by observer subjectivity.[8] Possible solutions that have been proposed include (1) semi-automated/automated point and shoot mapping[9] and (2) focal plane array (FPA) imaging.[10,11] Both of these methods are gaining popularity, although large datasets, expensive and specialized equipment, and sophisticated algorithms to assign polymer identity are currently hampering their wider uptake so far. Other technique-specific limitations include (a) poor-quality spectra resulting from colored particles using FTIR in transmission mode, (b) particle morphological artifacts when using FTIR in reflectance mode, and (c) fluorescence interference as a result of additives (e.g., pigments), or contaminants contained within or a biofilm surrounding the polymer while using Raman.[6,12] To alleviate these issues and provide alternatives for chemical characterization, various thermal techniques are becoming popular.

Although thermal analyses have been used for a number of years to characterize polymers, the move to identify plastic particles extracted from the environment is relatively new.[13] Benefits include the detection of plastics in complex matrices, without the need for extensive precleaning steps, and the reduction of possible interference caused by colored, fluorescent, and/or biofouled particles.[12−15] For example, polyethylene terephthalate (PET) was successfully detected in unprocessed standard loamy sand by thermogravimetric analysis-mass spectrometry (TGA-MS).[16] Dümichen et al.[17] detected polyethylene (PE) using a TGA analyzer connected to a solid-phase absorber that was subsequently analyzed by thermal extraction desorption-gas chromatography-mass spectroscopy (TED-GC-MS). The authors broadened their polymer library by including polypropylene (PP), polystyrene (PS), polyamide (PA), and PET, after which they successfully detected PE, PP, and PS in environmental samples.[18] Here, we aim to describe and investigate the capability of an alternative approach that incorporates many of the aforementioned techniques into a single instrument: thermogravimetric analysis-Fourier transform infrared-gas chromatography-mass spectrometry (TGA-FTIR-GC-MS, Figure S1), which collects physical and chemical information about a plastic particle to maximize the possibility of identifying the polymer type and any associated additives.

The first objective is to build a polymer library across each aspect of the platform to enable physical (TGA) and chemical (FTIR and GC-MS) characteristics to be collated. With this in place, the library is used to chemically characterize plastic particles in the size range of 1−5 mm originating from a single beach in the U.K. and from a citizen science campaign at three beaches in South Africa. Although researchers still refer to particles <5 mm as microplastics, here, we follow guidelines from Hartmann et al.[19] who stated that microplastic particles are less than 1 mm and mesoplastic particles fall between 1 and 10 mm, as there are clear methodological limitations for analysis of the submicrometer-sized particles.

MATERIALS AND METHODS

Source and Production of Polymers for the Plastic Library. Eleven polymer types, namely, PE, PP, PS and expanded polystyrene (EPS), PET, polyamide-6 (PA-6), both unplasticized and plasticized polyvinyl chloride (uPVC and pPVC), polycarbonate (PC), polymethyl methacrylate (PMMA), polytetrafluoroethylene (PTFE), polyurethane (PU), and polylactic acid (PLA), were used to build a library to be compared to data generated from the analysis of plastic particles extracted from environmental samples. These polymers were chosen due to availability either from household products, laboratory items, or industrially obtained pellets/powders. A total of 65 individual plastic samples were analyzed to produce the library. Initial identification of the polymers was through typical classification codes found on the item or product label. For more information, see Table S1. Additionally, a known PS standard, which was provided by the instrument manufacturer for calibration purposes, was run daily before any library samples or environmental samples were analyzed.

Thermogravimetric Analysis (TGA). All samples were analyzed using a TGA 8000 thermogravimetric analyzer (PerkinElmer, Waltham, MA, USA), which was controlled by the Pyris Software version 13.3.1.0019. Plastic samples were loaded into ceramic sample crucibles (PerkinElmer, U.K.), circa 6.6 mm in diameter and 1.95 mm in height, for pyrolytic decomposition. The temperature was held at 50 °C for 1 min then increased from 50 to 280 °C at 120 °C/min followed by a 12.5 °C/min increase to 700 °C under a nitrogen flow of 60 mL/min. To remove any residual mass that had not been pyrolyzed, each sample was exposed to an additional purging step where temperatures were ramped from 700 to 950 °C at 500 °C/min, at which point the gas flow was switched to an oxygen flow of 60 mL/min for 15 min. Cooling took place under a nitrogen flow of 60 mL/min, unless otherwise stated. By using the built-in step function, the onset, end, and inflection points were determined, and the % mass lost during each event was reported.

Fourier Transform Infrared Spectroscopy (FTIR). Around 90% of the evolved gas from the TGA analyzer entered the zero-gravity cell of a PerkinElmer Frontier FTIR spectrometer via a PerkinElmer TL9000 transfer line heated to 270 °C. At the beginning of each day, a blank was run using an empty ceramic sample crucible and a nitrogen flow of 60 mL/min. The blank scan ranged between 450 and 4000 cm^{-1} at a resolution of 8 cm^{-1} for 16 accumulations. For each sample, FTIR was triggered at 280 °C with a run time of 60 min. Data were collected continuously between 450 and 4000 cm^{-1} at a resolution of 8 cm^{-1} for 1 accumulation. All data were captured, and peak wavelengths were annotated using TimeBase version 3.1.6 (PerkinElmer, Waltham, MA, USA).

Gas Chromatography-Mass Spectrometry (GC-MS). The evolved gas passed from the zero-gravity FTIR cell through another PerkinElmer TL9000 transfer line set to 270 °C into a GC-MS instrument. The evolved gas was directed to waste until 50% of the sample weight had been lost, thereafter initiating a full-loop (100 μL) evolved gas slug injection into the inlet, which was set to 270 °C, of the GC-MS instrument. The subsequently evolved gas was directed to waste. A PerkinElmer Clarus 680 GC instrument was equipped with a PerkinElmer Elite 5 column (5% diphenyl−95% dimethyl polysiloxane, 30 m × 0.25 mm × 0.25 μm) at 40 °C, which was

https://doi.org/10.1021/acs.est.1c01085
Environ. Sci. Technol. XXXX, XXX, XXX−XXX

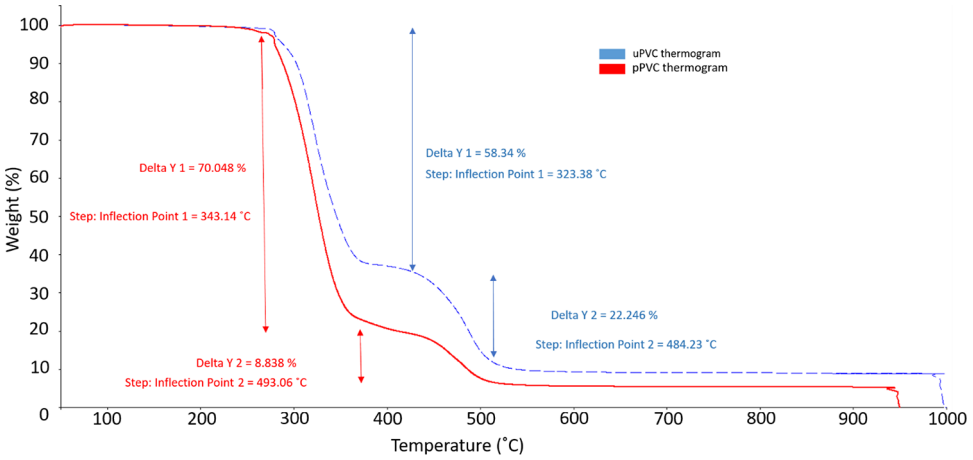

Figure 1. Overlaid thermograms of an examplary uPVC, the blue dashed line and text, and examplary pPVC, the red line and text, demonstrating the different thermal properties of these polymers. The differences in inflection points and mass loss are potentially a result of additives and fillers.

increased at 10 °C/min until 300 °C and maintained at this temperature for 5 min to clean the column. The carrier gas used was helium at a constant pressure of 12 psi. A single quadrupole PerkinElmer Clarus SQ 8T mass spectrometer was run with an EI source ionization energy of 70 eV. Mass spectral data was collected from 45 to 250 m/z (to avoid interference from permanent gases) for 31 min with a scan time of 0.25 s and an interscan delay of 0.05 s. The described parameters were used for all analyses unless otherwise stated. Mass spectra were compared against the NIST MS Search library V2.2 to identify evolved gas products. The GC-MS instrument was operated using TurboMass v6.1.0 (PerkinElmer, Waltham, MA, USA). The total length of the GC-MS method was designed to coincide with the end of the TGA analysis to increase sample throughput.

Environmental Samples. Thirteen suspected mesoplastics were removed by hand from a beach near Lowestoft (52°27′30.65″N; 1°44′29.17″E), Suffolk, U.K. Using a scalpel, a small fraction was removed for TGA-FTIR-GC-MS analysis. Additionally, small mesoplastics (between the size of 1 and 5 mm) were extracted from beach sediments at three locations, namely, Fish Hoek (34°08′26.2″S 18°25′56.3″E), Kommetjie (34°08′12.9″S 18°19′42.5″E), and Muizenberg (34°06′31.1″S 18°28′12.6″E), along the Cape Peninsula in the Western Cape Province of South Africa.

RESULTS AND DISCUSSION

Plastic Library. *Thermogravimetric Analysis (TGA).* The thermograms generated from the TGA data reveal three key data points. These features are (1) the inflection point, the temperature at which the rate of pyrolysis is the greatest, (2) the number of inflection points, and (3) the percentage of mass lost during pyrolysis. Each of these data points is useful to provide initial insights into the identity of a polymer.

Looking initially at the most commonly detected and/or identified plastics found in the environment, PS, PP, PE, PET, PA-6, and PU,[3] it is clear that TGA alone is not adequate to differentiate between these polymers. Both PP (n = 6, 4 sources) and PA-6 (n = 6, 2 sources) had very similar single inflection points at 479 ± 6 °C (mean ± SD) and 473 ± 2 °C and % mass losses of 97 ± 1 and 95 ± 1%, respectively. PS (n = 6, 3 sources) had a lower average single inflection point of 427 ± 5 °C, with a similar % mass loss of 96 ± 3% (Figure S2); this, however, was quite close to PU (n = 3, single source), which had an inflection point of 419 ± 5 °C. Although the mass lost was also similar at 95 ± 1%, PU appears to have a second pyrolysis step which is unfortunately difficult to distinguish (Figure S3). The inflection point for PET (n = 5, 4 sources) fell between that of PS and both PP and PA-6, with a single inflection point of 451 ± 1 °C (Figure S4). However, with only 82 ± 3% mass being pyrolyzed, the presence of residues, combined with this inflection point, may begin to distinguish PET from the other plastics investigated. Of these six polymers, PE (HDPE (n = 6, 2 sources) and LDPE (n = 7, 2 sources)) had the highest single inflection points of 501 ± 2 and 500 ± 2 °C with mass losses of 97 ± 2 and 96 ± 7%, respectively (Figures S5 and S6). As such, it is possible to get a putative identity of 3 of the 5 most frequently detected plastic contaminants by TGA alone when the polymers are analyzed individually. However, in all cases, additional information is required to conclusively identify the polymer.

In the case of the polymers less frequently identified in the environment, TGA may be particularly useful for assigning tentative identities. Of all the polymers characterized, uPVC (n = 3, 3 sources) and pPVC (n = 3, 3 sources) had the lowest inflection points of 311 ± 12 and 331 ± 11 °C (Figure S7), respectively. The wide variability between PVC samples is possibly a result of the source and/or the additive content.[20,21] All PVC samples had a distinctive second degradation stage with an inflection point at 481 ± 7 °C for uPVC and 487 ± 6 °C for pPVC, enabling them to be distinguished from the other polymers tested. The % mass losses for uPVC were 48 ± 10 and 19 ± 3% for the first and second inflection points, respectively, while pPVC lost 69 ± 1 and 9 ± 1% (Figure 1).

Aouachria et al.[22] described how the mass loss of PVC, in the first degradation stage, increased with increasing percentages of the di-2-ethylhexyl phthalate (DEHP) plasticizer. Looking at DEHP contents of 0, 15, 30, and 50%, Aouachria et al.[22] saw mass loss changes of 59.1, 64.2, 67.7, and 74.5%, respectively. Therefore, it may be possible to estimate the plasticizer percentage present in the uPVC sample shown in Figure 1 to be around 30%. This would need further investigation as other additives (i.e., lubricants, stabilizers, and flame retardants) are also known to have an effect on the inflection point and mass loss. For example, Matlack and Metzger[23] found that lubricants decreased the initial inflection point, while stabilizers had the opposite effect. Given the low

https://doi.org/10.1021/acs.est.1c01085
Environ. Sci. Technol. XXXX, XXX, XXX−XXX

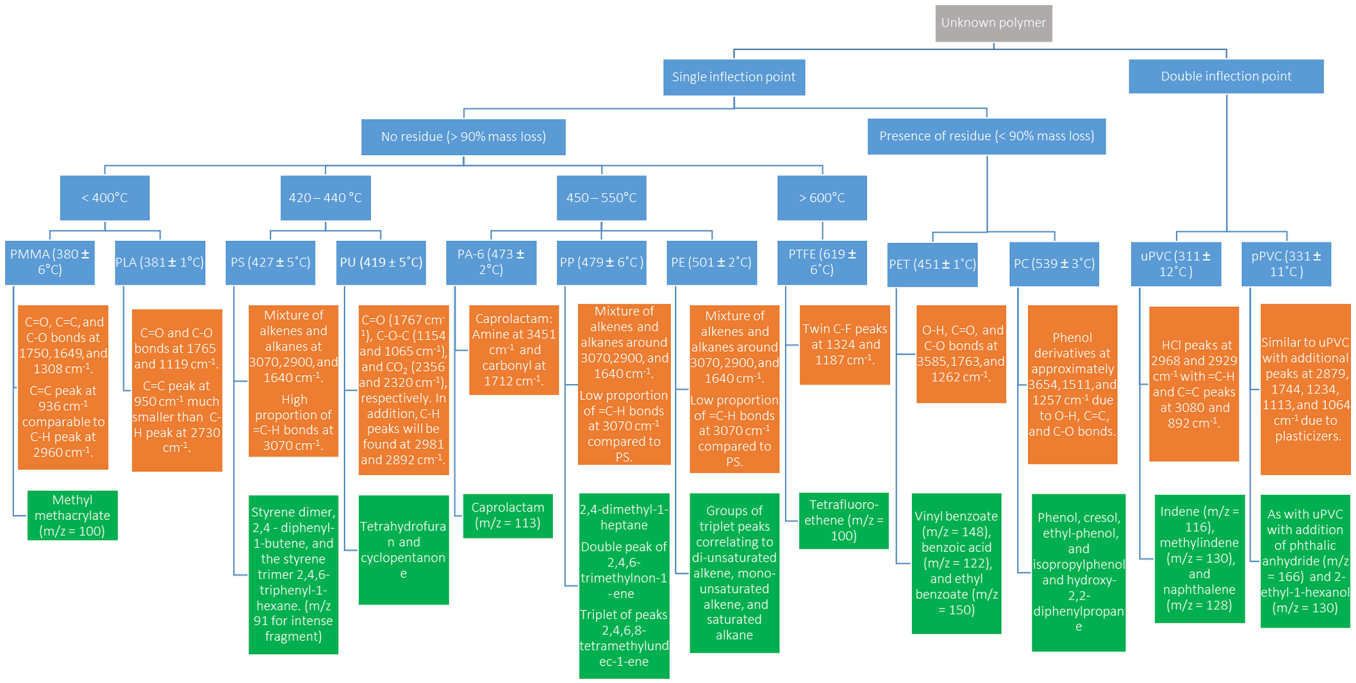

Figure 2. Decision tree for TGA (blue), FTIR (orange), and GC-MS (green) using the platform described in this study.

initial inflection point and the fact that there were two distinct pyrolysis events, PVC can be putatively identified by TGA.

PC (n = 6, 3 sources) with a relatively high inflection point of 539 ± 3 °C and a % mass loss of just 74 ± 1% (Figure S8) was the most distinctive among the polymers tested. Similar results have been seen in the literature, which showed large proportions of residues after pyrolysis.[24] Although residues were also a feature of PET degradation, there is an identifiable difference in their individual inflection points (Figure 2). PTFE (n = 6, 3 sources) may also be tentatively identified using the TGA thermogram as it had the highest inflection point of 619 ± 6 °C, 60 °C higher than the closest polymer, and a mass loss of more than 97 ± 3% (Figure S9). The final two polymers investigated, PMMA (n = 4, 2 sources) and PLA (n = 3, single source), displayed overlapping pyrolysis points with single-stage degradation events and inflection points of 380 ± 6 and 381 ± 1 °C, respectively (Figures S10 and S11). The amount of the material lost during pyrolysis was different (89 ± 6% vs 98 ± 1%); however, it would not be prudent to rely on a small change such as this, given that additives and fillers may influence the overall mass loss during pyrolysis. This may be the case for all polymers, and creation of an extensive library of polymers with a wide range of additives would require continued addition of samples and polymer types for analysis in the future. It should be noted that mixtures and copolymers were not investigated in the current study but should be included in future work.

Overall, the most common polymers found contaminating the environment could not be clearly characterized or distinguished from one another by TGA alone. However, some less common contaminants can be tentatively identified using exclusively TGA data.

Fourier Transform Infrared Spectroscopy (FTIR). The FTIR spectrum was used to identify different chemical bonds present within the evolved gas mixture and thus help to identify the polymer being analyzed. Unlike solid-phase FTIR, in this configuration, it is not the intact polymer being characterized but rather the pyrolysis compounds in the gas phase. This provides the potential benefit that several confounding factors such as the color, morphology, or fluorescence of the polymer that hamper solid-phase FTIR may be eliminated.

In contrast to the TGA data, differences between PA-6 and PP were easily identifiable due to the amine (N−H) peak present at 3451 cm^{-1} coupled with a carbonyl (C═O) peak at 1712 cm^{-1} indicative of caprolactam, a major pyrolysis product of PA-6 (Figure S12).[25] These two peaks make PA-6 distinctive from the other polymers analyzed.

PS, PP, and PE were difficult to differentiate, with the latter two being indistinguishable (Figures S13 and S14), given that they all pyrolyzed to produce a mixture of alkenes and alkanes. Each of these polymers produced peaks corresponding to alkenes (═C−H and C═C) and alkanes (−C−H) at wavelengths around 3070, 1640, and 2900 cm^{-1}, respectively, and therefore, FTIR peak identification could not distinguish between these materials. However, the PS spectra contained a higher proportion of alkene double bonds (C═C) due to the formation of styrene derivatives (Figure S15), whereas the pyrolyzed products of PE and PP contained mainly alkane (C−C) bonds. This was reflected in their respective spectra with a larger peak observed at 3070 cm^{-1} than at 2900 cm^{-1} for PS and the opposite seen with PE and PP.

The major pyrolysis product of uPVC is hydrochloric acid (HCl); however, this results in two peaks in the FTIR spectrum at approximately 2968 and 2929 cm^{-1}, making them indistinguishable from alkane C−H peaks (Figure S16). The other products formed are aromatic hydrocarbons creating ═C−H and C═C peaks at 3080 and 892 cm^{-1}, respectively. There were additional peaks observed in pPVC at 2879 (−C−H), 1744 (C═O), 1234 (C−O), 1113 (C−O), and 1064 (C−O) cm^{-1}, which may be a result of the plasticizer used (Figure S17). The high concentrations of HCl and potential additives can cause suppression of the aromatic hydrocarbon peaks (C═C and ═C−H). Although the spectra of uPVC and

https://doi.org/10.1021/acs.est.1c01085
Environ. Sci. Technol. XXXX, XXX, XXX−XXX

pPVC are easily distinguishable from each other, uPVC displays a similar spectrum to both PP and PE, and the pPVC spectrum is very similar to those of PMMA and PLA. This highlights the importance of combining this technique with TGA and GC-MS as both PVC polymers display a two-step degradation event that is not observed in the other materials.

PET, PC, PMMA, and PLA all pyrolyzed into products containing oxygen, carbon, and hydrogen; however, the bonding patterns of these atoms allowed the polymers to be identified. Pyrolysis of PET into benzoic acid, ethyl benzoic acid, and vinyl benzoate[18,26] resulted in a combination of peaks at approximately 3585, 1763, and 1262 cm^{-1} due to the O−H, C═O, and C−O bonds, respectively (Figure S18). PC pyrolyzed into phenol derivatives[18,26] all characterized by peaks at approximately 3654, 1511, and 1257 cm^{-1} corresponding to O−H, C═C, and C−O bonds (Figure S19). PMMA pyrolyzed into its monomer, methyl methacrylate, with C═O, C═C, and C−O bonds displaying peaks at approximately 1750, 1649, and 1308 cm^{-1}, respectively (Figure S20). The pyrolysis products of PLA are acetaldehyde, 2,3-pentadione, acrylic acid, and lactide, which produce similar peaks to those observed with PMMA; however, the ratio of C═C bonds to C−H, C═O, and C−O bonds was greatly reduced causing suppression of the peak heights (Figure S21) at approximately 3000 and 950 cm^{-1}.

PTFE revealed the most distinctive spectrum with two large peaks observed, at approximately 1324 and 1187 cm^{-1}, corresponding to the C−F bonds in the fluorinated alkene pyrolysis products (Figure S22). Polyurethanes are copolymers synthesized from the reaction of di-isocyanates with polyols creating an amide linkage. There is a large variety of polyurethanes, and their properties depend on the two monomers used. This variety makes identification by FTIR difficult as there is no single unique spectrum. During pyrolysis, the isocyanate segments decompose over a short temperature range at relatively low temperatures, and as a result, only the polyol degradation products can be found in the associated FTIR spectrum. The main pyrolysis products of the polyol units are cyclic ketones such as cyclopentanone, cyclic ethers such as tetrahydropyran, and carbon dioxide. These compounds result in peaks corresponding to C═O (1767 cm^{-1}), C−O−C (1154 and 1065 cm^{-1}), and CO_2 (2356 and 2320 cm^{-1}), respectively. In addition, C−H peaks can be found at 2981 and 2892 cm^{-1} (Figure S23).

Gas Chromatography-Mass Spectrometry (GC-MS). GC separates the complex chemical mixture of the evolved gas and analytes, which are subsequently detected using the EI mass spectrometer. Due to the complex mixture of chemicals in the evolved gas, each polymer sample results in the detection of multiple peaks. In many cases, common peaks are detected across multiple polymers. For example, styrene, toluene, and benzene are common pyrolysis products across multiple polymers and therefore cannot be used to confirm identity. Here, we focus on the unique peaks required for definitive polymer identification.

The additional chemical characterization by GC-MS allowed PP, PS, and PE to be differentiated. The GC-MS spectrum for PP contained several distinguishing peaks enabling a firm polymer identity to be assigned (Figure S24). The first distinctive peak is 2,4-dimethyl-1-heptene eluted at 4.7 min followed by the meso and racemic isomers of 2,4,6-trimethylnon-1-ene and finally the triplet of peaks associated with isotactic, heterotactic, and syndiotactic 2,4,6,8-tetramethylundec-1-ene.[13,18,26] These peaks have been previously reported as key in the identification of PP, though standards for each chemical are required to definitively identify specific chiral isomers. The production of alkenes and alkanes during pyrolysis supports the findings of FTIR, while their specificity allows PP to be distinguished from PS and PE. In the case of PE, a repeated pattern of triplet peaks could be seen in the mass spectrum (Figure S25). Starting at 5.3 min, it was possible to detect groups of triplet peaks correlating to di-unsaturated alkenes, mono-unsaturated alkenes, and saturated alkanes with the same carbon count.[13,17,26−28] This triplet pattern reflects the β-scission of further CH_2 groups resulting in a mass loss of 14 Da between triplets, with the later eluted peaks having longer polymer chain lengths. This repeated triplet peak was unique to PE and visible in the total ion chromatograms (TIC) for larger particles or in the extracted ion chromatograms, using the fragment masses of 55 and 57 Da. Defining characteristic peaks for PS was more difficult. The main pyrolysis peak was for the monomer styrene, which is a common pyrolysis product among the polymers tested. However, this peak was larger and correlated to the larger styrene derivative peaks in the FTIR spectra. Using a PS chip (8.2 mg), it was possible to identify the styrene dimer, 2,4-diphenyl-1-butene, and the styrene trimer 2,4,6-triphenyl-1-hexene, both of which were unique to PS (Figure S26).[13,18,26,29] However, the trimer could only be seen when the most intense fragments (m/z 91, 115, 130, and 193 at 24.8 min) were searched for. With less dense EPS, a lower mass could be loaded onto the crucible, and thus, only the common peaks for toluene, benzene, styrene, and methyl styrene could be easily detected. In real environmental samples, this poses a significant hurdle as EPS is a common contaminant and the current method is poorly suited for definitive identification of EPS.

As with many previous studies,[13,18,26,30] PA-6 was easily identifiable due to the presence of caprolactam (Figure S27), the monomer of PA-6 that undergoes ring-opening polymerization. Upon pyrolysis, PA-6 undergoes homolytic chain scission to reform the monomer. Indeed, this has been investigated as a potential mechanism to recover caprolactam from waste PA-6.[31] This peak was unique to PA-6; however, other nylons such as PA-6,6 and Nylon-MXD6 may also form caprolactam upon pyrolysis though to a lesser extent.[26]

PET was identified by the presence of vinyl benzoate at 6.67 min, benzoic acid at 9.72 min, and ethyl benzoate at 9.96 min, all of which were found to be unique to PET in this study (Figure S28). The consumer item, glitter, was also examined and showed the same three indicative pyrolysis products found in our reference PET fragments but with the addition of phthalic anhydride at 12.2 min and divinyl terephthalate at 15.58 min.[13,18,26,32] Phthalic anhydride is used in the manufacture of plasticizers, certain pigments, and dyes.

The two PVC polymers, uPVC and pPVC, both pyrolyzed to produce three peaks that are widely used in pyGC-MS as indicated, indene (retention time (rt) = 12.3 min), methylindene (rt = 9.95 min), and naphthalene (rt = 10.3 min) (Figure S29), representing the cyclization event occurring as dechlorination during pyrolysis.[26,33] Interestingly, additional peaks were detected in the pPVC chromatogram, namely, phthalic anhydride (rt = 12.3 min) and 2-ethyl-1-hexanol (rt = 7.69 min), both of which are precursors of the phthalate DEHP and may have been produced via de-

https://doi.org/10.1021/acs.est.1c01085
Environ. Sci. Technol. XXXX, XXX, XXX−XXX

esterification during the pyrolysis process. The presence of these DEHP precursors supports the previous discrepancy seen between uPVC and pPVC in the TGA and FTIR results and lends credence to the theory that the presence of plasticizers can be detected, especially in TGA as previously mentioned. The detection of these phthalates in pPVC and PET (phthalic anhydride) demonstrates a key advantage of using this TGA-FTIR-GC-MS platform. The ability to detect these DEHP pyrolysis products and potentially other additives may also be of use to investigate compliance with government bans on the use of these endocrine-disrupting chemicals in certain products.[34]

The PC samples were distinctive among the polymers evaluated due to the abundance of phenolic pyrolysis products; as seen in the FTIR spectrum, these included phenol, cresol, ethyl-phenol, and isopropylphenol (Figure S30).[26] These and hydroxy-2,2-diphenylpropane (rt = 16.9 min) are pyrolysis products of Bisphenol A (BPA); the lack of a BPA peak, which is commonly seen in pyGC-MS, may be due to a more complete pyrolysis here, resulting in less BPA monomer being present in the evolved gas.

Both PMMA and PTFE pyrolyzed to their respective monomers, methyl methacrylate (rt = 3.34 min) and tetrafluoro-ethene (rt = 2.14 min) (Figure S31). Although both methyl methacrylate and tetrafluoro-ethene have the same nominal mass of 100 Da, their fragmentation patterns and retention times are sufficiently different to differentiate between the two. PU was distinctive based upon two peaks in the GC-MS spectra, namely, tetrahydrofuran (rt = 2.77 min) and cyclopentanone (rt = 4.08 min) (Figure S32), making it distinguishable from PS with which it shares common TGA characteristics (Figure 2). The final polymer tested, PLA, did not reveal any key identifying peaks in the GC-MS chromatogram due to the main pyrolysis product being acetaldehyde, which has a mass of 44 Da and falls below the scanned range used in this method.[26] The ability to characterize PLA would require selected ion monitoring to reduce background noise at the low mass range and to detect the parent compound m/z = 44 and expected fragment at m/z = 29.

Environmental Validation. In order to reduce misidentification, it was decided that a definitive identity would only be given where all three instruments could be used to narrow down the polymer identity.

United Kingdom Samples. Using the decision tree shown in Figure 2, 12 suspected plastic particles were successfully assigned a polymer identity, with a single specimen remaining unknown. PE was the most dominant polymer type (n = 7) followed by both PP (n = 2) and PS (n = 2). PVC occurred only once among the 12 fragments tested.

As expected on the basis of differences in additives, inflection points of the environmental plastic fragments varied compared to their reference library counterparts. Inflection points of PE, which according to the reference plastic library were 496−503 °C, ranged between 488 and 509 °C for the environmental samples. Although these are still distinguishable, the lower the inflection point, the more it may overlap with PP and PA-6. Interestingly, a flexible PVC piece was confirmed as it showed a second inflection point at 492 °C. The first inflection point at 278 °C was lower than previously recorded (331 ± 11 °C), which may be due to variable additive amounts and types. With a mass loss of 71% in the first degradation step, the presence of the DEHP plasticizer may be as high as 50% in this sample,[22] although this is speculative and would need to be investigated further.

The FTIR analysis of the evolved gas alone was unable to distinguish between PE and PP due to overlapping alkene and alkane peaks in the spectra (Table S2), but the lack of other distinguishing peaks was able to rule out the other 9 polymers from the library. In the case of the PS fragments, FTIR was able to distinguish from PU, which also has pyrolysis features similar to those of PS (Figure 2).

Clear indicative GC-MS peaks allowed the confirmation of all PE, PP, and PVC fragments. Although large styrene and methyl styrene peaks were seen in two fragments, which were suggested to be PS by FTIR previously, the dimer was present as a small peak in both samples, and the trimer was only detected in one of the samples. Peaks suggesting the presence of phthalic anhydride and 2-ethyl-1-hexanol appeared in the PVC spectrum, the presence of which is supported by a mass loss of 71% during pyrolysis; however, these peaks were not as intense as in the reference material. This may be a consequence of aging and weathering, as plasticizers leach out of plastics over time as they are not covalently bound to the polymer.

South African Samples. In total, 23 particles were analyzed from three South African beaches, i.e., Kommetjie (n = 1), Muizenberg (n = 4), and Fish Hoek (n = 18). This in part reflects the distribution of suspected plastic particles across the three beaches, with higher densities recorded at Fish Hoek (172−176 particles m^{-2} in May 2019) and Muizenberg, (60−216 particles m^{-2} in June/July 2019). Kommetjie, situated on the Atlantic Seaboard, had the lowest plastic contamination recorded in both May and June/July, with particles only found at the end of the beach zone.

Not all 23 particles were assigned a polymer identity according to the Figure 2 decision tree. Nine were definitively identified, 11 were given a tentative identity, and three remained unknown as shown in Table S3. PE appeared as the most dominant polymer (n = 16, of which 7 were confirmed across the whole platform, i.e., from TGA, FTIR, and GC-MS), with PP definitively identified twice. Of the 11 particles assigned a tentative identity, evidence suggested that 9 of the particles were most likely PE, with the others tentatively identified as PS and polymethylstyrene (Table S3). Overall, some interesting variations emerged that may highlight the physical and chemical changes that plastic particles undergo in the natural environment due to weathering and mechanical abrasion. Additionally, these variations display the complexities faced when assigning polymer identity to unknown environmental particles and the need for a multiplatform technique.

In most of the cases, FTIR identification of the polymer was inconclusive as the pyrolyzed forms of PE and PP are indistinguishable. Regardless, FTIR was beneficial to narrowing down the options given by the TGA data. GC-MS confirmed the identity tentatively assigned using TGA and FTIR data. Interestingly, although polymer chain shortening (sequential loss of CH_2) is indicative of PE, there was evidence of slight variations between PE particles extracted from the environment. For example, GC-MS confirmed the identity of Muizenberg particles 1−3 as PE; however, particle 3 had peaks for the CH_2 chain from C14 to C22, which may suggest that within the environment, the polymer has oxidized forming stronger bonds that may reduce the formation of these small polymer chains.[35] Results may also be due to various forms of PE having differing degrees of branching, thus leading to

https://doi.org/10.1021/acs.est.1c01085
Environ. Sci. Technol. XXXX, XXX, XXX−XXX

different pyrolysis products being detected by GC-MS although remaining undistinguishable by TGA-FTIR.[36]

Due to its low density, EPS is difficult to characterize as the volume to mass ratio is low, meaning that less sample is loaded anytime. However, when combined with morphological characteristics, an identity was assigned. For example, particle 11 extracted from Fish Hoek physically resembled EPS. An inflection point of 423 °C and high mass loss during pyrolysis suggested that the polymer could be PS. FTIR, however, was unable to further narrow this down with PE, PP, and PS being possible outcomes. Due to the small sample mass, the dimer and trimer were not detected by GC-MS. The styrene peak dominated the spectrum; therefore, a combination of physical and chemical information suggested that this particle was composed of PS. Moving forward, the integration of two short selected ion monitoring segments at 17.5 and 24.9 min, ±20 s, in the MS method to overlap with the expected retention time of the dominant fragment peaks of the dimer and trimer may improve sensitivity and allow confirmation of EPS versus PS.

Nine other particles were tentatively assigned a chemical identity of PE; however, the GC-MS spectra contained no peaks or very few peaks with only hexane at 2.65 min being detected. The TGA inflection point and % mass loss were indicative of PE, while FTIR suggested either PE or PP. This variation could be a result of color, biofouling, and/or weathering, altering the mass loss profile, meaning that the trigger for GC-MS at 50% mass loss could miss the indicative compounds in the evolved gas, but this is unclear and would need further experimental work to evaluate.

The final tentative polymer identification highlights the benefit of this platform's untargeted approach to polymer characterization. Fish Hoek particle 15 was presented as a pale orange fragment 4 × 3 mm in size; upon pyrolysis, a single inflection point was observed at 474.4 °C, which initially suggests PP; however, upon GC-MS analysis, the indicative peaks of PP were not present, and instead, an intense methyl styrene peak was observed (rt = 6.86 min, m/z = 118) alongside xylene (rt = 5.03 min, m/z = 106), benzaldehyde (rt = 5.95 min, m/z = 106), and 2-phenylpropenal (rt = 7.51 min, m/z = 132) in addition to the common pyrolysis products styrene, toluene, and benzene. These peaks are indicative of the polymer being polymethylstyrene.[26] Interestingly, this polymer was detected by Vilakati et al.[37] when analyzing Neuston net samples collected from locations in Cape Town, South Africa.

Three particles, one from Muizenberg and two from Fish Hoek, yielded inconclusive results. The TGA data for the particle from Muizenberg did not match any of the library polymers. The FTIR signal was too weak to ascertain any definitive peaks, and GC-MS was only able to detect a styrene peak. The inability to assign a polymer identification could be due to a number of factors: the polymer may not be included yet in the in-house reference library, or the mass, 0.422 mg for this particular polymer, was too low. An orange particle from Fish Hoek (particle 7) had an inflection point similar to that of PP or PA-6. The FTIR signal suggested either PE or PP, implying that a chemical identity of PP could be assigned. However, styrene, toluene, indene, ethylbenzene, and xylene were detected by GC-MS. Indene may suggest PVC, while ethylbenzene and xylene may suggest PC. Styrene and toluene are present in both and are not considered as indicative peaks. Another example was a spherical black particle from Fish Hoek, which did not trigger a GC-MS run as it did not lose 50% of its mass during pyrolysis, therefore ruling out all polymers in the library.

Environmental Implications and Future Directions. The current setup triggers GC-MS at 50% mass loss, which allows for an untargeted analysis as no a priori knowledge of the polymer type is available. This, however, means that the method is qualitative as the 50% mass loss trigger is influenced by the additive content or the nonpolymer material in unprocessed samples. This leaves potential for some chemical information to be lost; thus, key additives or polymer markers may not be definitively identified. While it would be possible to quantify by MS if GC was bypassed, this would, however, reduce confidence in polymer identification through loss of chromatographic separation. The loss of chromatographic concentration may also reduce overall sensitivity. Future work would benefit from investigating the prospect of trapping the evolved gas after FTIR analysis and then performing GC-MS analysis.[38,39] This would enable the incorporation of internal standards for quantification and maximize sensitivity while potentially allowing the analysis of unprocessed samples from the environment.[16] To increase confidence in GC-MS identifications and increase the mass resolution between compounds of the same nominal mass, hyphenation to high-resolution mass spectrometers could be a future step. These provide <5 ppm mass accuracy. In the case of PLA, the pyrolysis product has a mass of 44 Da, which is identical to that of CO_2; accurate mass measurement will resolve these two peaks in the mass spectra. While the present work is qualitative, it offers an improvement on previous work where each technique is used separately or hyphenated to a single other technique. This three-way combination enables a broader chemical space to be characterized with the addition of physical property analysis without the additional cost of splitting a sample between techniques or of additional analysis time. This study provides the foundation for future work that will look to expand this library to encompass other key polymers and copolymers such as additional polyamides, acrylonitrile-butadiene styrene, ethylene-vinyl acetate, and styrene-butadiene rubber, in addition to investigating composites, for example, polymers with nonpolymer fillers/reinforcements. This may be particularly interesting with the current strength of TGA to detect changes in additive and filler contents. In addition, the library should be extended to cover different molecular weights for the same polymer as it is possible that some of the variations seen in the TGA inflection points may reflect differences in molecular weight. Furthermore, future work could also look to quantify any metal species present by ICP-MS in the residual mass following pyrolysis as this could provide interesting information of additives such as colorants in samples. It would also be beneficial to investigate how this method is applicable for special cases such as surface coatings and tire wear particles.[19]

■ ASSOCIATED CONTENT

Supporting Information

The Supporting Information is available free of charge at https://pubs.acs.org/doi/10.1021/acs.est.1c01085.

Paragraph detailing the collection of mesoplastics in South Africa; Table S1 detailing the source of plastics used to generate the library; two tables (Tables S2 and S3) providing information about the mesoplastics analyzed across the TGA-FTIR-GC-MS platform;

https://doi.org/10.1021/acs.est.1c01085
Environ. Sci. Technol. XXXX, XXX, XXX−XXX

schematic of the TGA-FTIR-GC-MS platform (Figure S1); thermograms of each plastic analyzed; FTIR spectrum of each plastic analyzed; and GC-MS total ion chromatogram of each plastic analyzed (PDF)

AUTHOR INFORMATION

Corresponding Author

Holly A. Nel − *School of Geography, Earth and Environmental Sciences, University of Birmingham, Birmingham B15 2TT, United Kingdom;* orcid.org/0000-0002-0571-2678; Email: h.a.nel@bham.ac.uk

Authors

Andrew J. Chetwynd − *School of Geography, Earth and Environmental Sciences, University of Birmingham, Birmingham B15 2TT, United Kingdom;* orcid.org/0000-0001-6648-6881

Catherine A. Kelly − *School of Metallurgy and Materials, University of Birmingham, Birmingham B15 2TT, United Kingdom*

Christopher Stark − *School of Geography, Earth and Environmental Sciences, University of Birmingham, Birmingham B15 2TT, United Kingdom*

Eugenia Valsami-Jones − *School of Geography, Earth and Environmental Sciences, University of Birmingham, Birmingham B15 2TT, United Kingdom;* orcid.org/0000-0002-8850-7556

Stefan Krause − *School of Geography, Earth and Environmental Sciences, University of Birmingham, Birmingham B15 2TT, United Kingdom; LEHNA—Laboratoire d'Ecologie des Hydrosystèmes Naturels et Anthropisés, University of Lyon, Lyon 69007, France*

Iseult Lynch − *School of Geography, Earth and Environmental Sciences, University of Birmingham, Birmingham B15 2TT, United Kingdom;* orcid.org/0000-0003-4250-4584

Complete contact information is available at: https://pubs.acs.org/10.1021/acs.est.1c01085

Author Contributions

‖H.A.N. and A.J.C. contributed equally to the article.

Funding

This work was funded by the Leverhulme Trust grant "PlasticRivers" (RPG-2017-377; S.K., I.L., and H.A.N.) and from the European Commission via the Horizon2020 project ACEnano (grant no. H2020-NMBP-2016-720952; E.V.-J., I.L., A.J.C., and C.S.).

Notes

The authors declare no competing financial interest.

ACKNOWLEDGMENTS

The authors would like to dedicate this paper to Sara King, the cofounder of Evolve Abroad who passed away in a tragic accident in 2019. Evolve Abroad (https://evolveabroad.com/) and their students collected plastic particles from South African beaches, which formed the basis of this study's environmental relevance section. The authors would also like to express their gratitude to Gerlinde Wita, John Attwood, and Aaron Davis from PerkinElmer for making the software available for use during the 2019−2020 Covid19 virus outbreak, enabling us to continue this work from home under social distancing measures. The authors would like to thank the editors and the three reviewers for their time and effort to evaluate the work and their constructive comments that greatly improved the manuscript.

REFERENCES

(1) Ballent, A.; Corcoran, P. L.; Madden, O.; Helm, P. A.; Longstaffe, F. J. Sources and sinks of microplastics in Canadian Lake Ontario nearshore, tributary and beach sediments. *Mar. Pollut. Bull.* **2016**, *110*, 383−395.

(2) Drummond, J. D.; Nel, H. A.; Packman, A. I.; Krause, S. Significance of Hyporheic Exchange for Predicting Microplastic Fate in Rivers. *Environ. Sci. Technol. Lett.* **2020**, *7*, 727−732.

(3) Erni-Cassola, G.; Zadjelovic, V.; Gibson, M. I.; Christie-Oleza, J. A. Distribution of plastic polymer types in the marine environment; A meta-analysis. *J. Hazard. Mater.* **2019**, *369*, 691−698.

(4) Cowger, W.; Booth, A. M.; Hamilton, B. M.; Thaysen, C.; Primpke, S.; Munno, K.; Lusher, A. L.; Dehaut, A.; Vaz, V. P.; Liboiron, M.; Devriese, L. I.; Hermabessiere, L.; Rochman, C.; Athey, S. N.; Lynch, J. M.; De Frond, H.; Gray, A.; Jones, O. A. H.; Brander, S.; Steele, C.; Moore, S.; Sanchez, A.; Nel, H. Reporting Guidelines to Increase the Reproducibility and Comparability of Research on Microplastics. *Appl. Spectrosc.* **2020**, *74*, 1066−1077.

(5) Hahladakis, J. N.; Velis, C. A.; Weber, R.; Iacovidou, E.; Purnell, P. An overview of chemical additives present in plastics: Migration, release, fate and environmental impact during their use, disposal and recycling. *J. Hazard. Mater.* **2018**, *344*, 179−199.

(6) Xu, J.-L.; Thomas, K. V.; Luo, Z.; Gowen, A. A. FTIR and Raman imaging for microplastics analysis: State of the art, challenges and prospects. *TrAC, Trends Anal. Chem.* **2019**, *119*, 115629.

(7) Song, Y. K.; Hong, S. H.; Jang, M.; Han, G. M.; Rani, M.; Lee, J.; Shim, W. J. A comparison of microscopic and spectroscopic identification methods for analysis of microplastics in environmental samples. *Mar. Pollut. Bull.* **2015**, *93*, 202−209.

(8) Nel, H. A.; Chetwynd, A. J.; Kelleher, L.; Lynch, I.; Mansfield, I.; Margenat, H.; Onoja, S.; Goldberg Oppenheimer, P.; Sambrook Smith, G. H.; Krause, S. Detection limits are central to improve reporting standards when using Nile red for microplastic quantification. *Chemosphere* **2021**, *263*, 127953.

(9) Frere, L.; Paul-Pont, I.; Moreau, J.; Soudant, P.; Lambert, C.; Huvet, A.; Rinnert, E. A semi-automated Raman micro-spectroscopy method for morphological and chemical characterizations of microplastic litter. *Mar. Pollut. Bull.* **2016**, *113*, 461−468.

(10) Tagg, A. S.; Sapp, M.; Harrison, J. P.; Ojeda, J. J. Identification and Quantification of Microplastics in Wastewater Using Focal Plane Array-Based Reflectance Micro-FT-IR Imaging. *Anal. Chem.* **2015**, *87*, 6032−6040.

(11) Mintenig, S. M.; Int-Veen, I.; Löder, M. G. J.; Primpke, S.; Gerdts, G. Identification of microplastic in effluents of waste water treatment plants using focal plane array-based micro-Fourier-transform infrared imaging. *Water Res.* **2017**, *108*, 365−372.

(12) Shim, W. J.; Hong, S. H.; Eo, S. E. Identification methods in microplastic analysis: a review. *Anal. Methods* **2017**, *9*, 1384−1391.

(13) Fischer, M.; Scholz-Böttcher, B. M. Simultaneous Trace Identification and Quantification of Common Types of Microplastics in Environmental Samples by Pyrolysis-Gas Chromatography−Mass Spectrometry. *Environ. Sci. Technol.* **2017**, *51*, 5052−5060.

(14) Käppler, A.; Fischer, M.; Scholz-Böttcher, B. M.; Oberbeckmann, S.; Labrenz, M.; Fischer, D.; Eichhorn, K.-J.; Voit, B. Comparison of μ-ATR-FTIR spectroscopy and py-GCMS as identification tools for microplastic particles and fibers isolated from river sediments. *Anal. Bioanal. Chem.* **2018**, *410*, 5313−5327.

(15) Okoffo, E. D.; Ribeiro, F.; O'Brien, J. W.; O'Brien, S.; Tscharke, B. J.; Gallen, M.; Samanipour, S.; Mueller, J. F.; Thomas, K. V. Identification and quantification of selected plastics in biosolids by pressurized liquid extraction combined with double-shot pyrolysis gas chromatography−mass spectrometry. *Sci. Total Environ.* **2020**, *715*, 136924.

(16) David, J.; Steinmetz, Z.; Kučerík, J.; Schaumann, G. E. Quantitative Analysis of Poly(ethylene terephthalate) Microplastics in Soil via Thermogravimetry−Mass Spectrometry. *Anal. Chem.* **2018**, *90*, 8793−8799.
(17) Dümichen, E.; Barthel, A.-K.; Braun, U.; Bannick, C. G.; Brand, K.; Jekel, M.; Senz, R. Analysis of polyethylene microplastics in environmental samples, using a thermal decomposition method. *Water Res.* **2015**, *85*, 451−457.
(18) Dümichen, E.; Eisentraut, P.; Bannick, C. G.; Barthel, A.-K.; Senz, R.; Braun, U. Fast identification of microplastics in complex environmental samples by a thermal degradation method. *Chemosphere* **2017**, *174*, 572−584.
(19) Hartmann, N. B.; Hüffer, T.; Thompson, R. C.; Hassellöv, M.; Verschoor, A.; Daugaard, A. E.; Rist, S.; Karlsson, T.; Brennholt, N.; Cole, M.; Herrling, M. P.; Hess, M. C.; Ivleva, N. P.; Lusher, A. L.; Wagner, M. Are We Speaking the Same Language? Recommendations for a Definition and Categorization Framework for Plastic Debris. *Environ. Sci. Technol.* **2019**, *53*, 1039−1047.
(20) Jia, P.; Hu, L.; Feng, G.; Bo, C.; Zhang, M.; Zhou, Y. PVC materials without migration obtained by chemical modification of azide-functionalized PVC and triethyl citrate plasticizer. *Mater. Chem. Phys.* **2017**, *190*, 25−30.
(21) Xu, J.; Liu, C.; Qu, H.; Ma, H.; Jiao, Y.; Xie, J. Investigation on the thermal degradation of flexible poly(vinyl chloride) filled with ferrites as flame retardant and smoke suppressant using TGA−FTIR and TGA−MS. *Polym. Degrad. Stab.* **2013**, *98*, 1506−1514.
(22) Aouachria, K.; Quintard, G.; Massardier-Nageotte, V.; Belhaneche-Bensemra, N. The effect of di-(−2-ethyl hexyl) phthalate (Dehp) as plasticizer on the thermal and mechanical properties of pvc/pmma blends. *Polímeros* **2014**, *24*, 428−433.
(23) Matlack, J. D.; Metzger, A. P. Thermal stability of modified poly(vinyl chloride) by TGA. *J. Appl. Polym. Sci.* **1968**, *12*, 1745−1750.
(24) Jang, B. N.; Wilkie, C. A. A TGA/FTIR and mass spectral study on the thermal degradation of bisphenol A polycarbonate. *Polym. Degrad. Stab.* **2004**, *86*, 419−430.
(25) Bradley, E. L.; Speck, D. R.; Read, W. A.; Castle, L. Method of test and survey of caprolactam migration into foods packaged in nylon-6. *Food Addit. Contam.* **2004**, *21*, 1179−1185.
(26) Shin, T.; Hajime, O.; Chuichi, W., *Pyrolysis-GC/MS Data Book of Synthetic Polymers: Pyrograms, Thermograms and MS of Pyrolyzates*. 2011; p 1−390.
(27) Rizzarelli, P.; Rapisarda, M.; Perna, S.; Mirabella, E. F.; La Carta, S.; Puglisi, C.; Valenti, G. Determination of polyethylene in biodegradable polymer blends and in compostable carrier bags by Py-GC/MS and TGA. *J. Anal. Appl. Pyrolysis* **2016**, *117*, 72−81.
(28) Soják, L.; Kubinec, R.; Jurdáková, H.; Hájeková, E.; Bajus, M. High resolution gas chromatographic−mass spectrometric analysis of polyethylene and polypropylene thermal cracking products. *J. Anal. Appl. Pyrolysis* **2007**, *78*, 387−399.
(29) Funck, M.; Yildirim, A.; Nickel, C.; Schram, J.; Schmidt, T. C.; Tuerk, J. Identification of microplastics in wastewater after cascade filtration using Pyrolysis-GC−MS. *MethodsX* **2020**, *7*, 100778.
(30) Fries, E.; Dekiff, J. H.; Willmeyer, J.; Nuelle, M.-T.; Ebert, M.; Remy, D. Identification of polymer types and additives in marine microplastic particles using pyrolysis-GC/MS and scanning electron microscopy. *Environ. Sci.: Processes Impacts* **2013**, *15*, 1949−1956.
(31) Czernik, S.; Elam, C. C.; Evans, R. J.; Meglen, R. R.; Moens, L.; Tatsumoto, K. Catalytic pyrolysis of nylon-6 to recover caprolactam. *J. Anal. Appl. Pyrolysis* **1998**, *46*, 51−64.
(32) Brems, A.; Baeyens, J.; Vandecasteele, C.; Dewil, R. Polymeric Cracking of Waste Polyethylene Terephthalate to Chemicals and Energy. *J. Air Waste Manage. Assoc.* **2011**, *61*, 721−731.
(33) Zhou, J.; Gui, B.; Qiao, Y.; Zhang, J.; Wang, W.; Yao, H.; Yu, Y.; Xu, M. Understanding the pyrolysis mechanism of polyvinyl-chloride (PVC) by characterizing the chars produced in a wire-mesh reactor. *Fuel* **2016**, *166*, 526−532.
(34) Erythropel, H. C.; Maric, M.; Nicell, J. A.; Leask, R. L.; Yargeau, V. Leaching of the plasticizer di(2-ethylhexyl)phthalate (DEHP) from plastic containers and the question of human exposure. *Appl. Microbiol.* **2014**, *98*, 9967−9981.
(35) Bonhomme, S.; Cuer, A.; Delort, A. M.; Lemaire, J.; Sancelme, M.; Scott, G. Environmental biodegradation of polyethylene. *Polym. Degrad. Stab.* **2003**, *81*, 441−452.
(36) Eselem Bungu, P. S.; Pasch, H. Comprehensive analysis of branched polyethylene: the multiple preparative fractionation concept. *Polym. Chem.* **2017**, *8*, 4565−4575.
(37) Vilakati, B.; Sivasankar, V.; Mamba, B. B.; Omine, K.; Msagati, T. A. M. Characterization of plastic micro particles in the Atlantic Ocean seashore of Cape Town, South Africa and mass spectrometry analysis of pyrolyzate products. *Environ. Pollut.* **2020**, *265*, 114859.
(38) Costache, M. C.; Jiang, D. D.; Wilkie, C. A. Thermal degradation of ethylene−vinyl acetate coplymer nanocomposites. *Polymer* **2005**, *46*, 6947−6958.
(39) Duemichen, E.; Eisentraut, P.; Celina, M.; Braun, U. Automated thermal extraction-desorption gas chromatography mass spectrometry: A multifunctional tool for comprehensive characterization of polymers and their degradation products. *J. Chromatogr. A* **2019**, *1592*, 133−142.

https://doi.org/10.1021/acs.est.1c01085
Environ. Sci. Technol. XXXX, XXX, XXX−XXX